Taylor & Francis
Taylor & Francis Group

Phosphorus, Sulfur, and Silicon and the Related Elements

ISSN: 1042-6507 (Print) 1563-5325 (Online) Journal homepage: www.tandfonline.com/journals/gpss20

New 2-hydrazinothiazole derivatives as potential MAO-A, MAO-B, AChE, and BChE inhibitors

Beyzanur Tutuş, Asaf Evrim Evren, Begüm Nurpelin Sağlik Özkan & Leyla Yurttaş

To cite this article: Beyzanur Tutuş, Asaf Evrim Evren, Begüm Nurpelin Sağlik Özkan & Leyla Yurttaş (2024) New 2-hydrazinothiazole derivatives as potential MAO-A, MAO-B, AChE, and BChE inhibitors, Phosphorus, Sulfur, and Silicon and the Related Elements, 199:10-12, 864-875, DOI: 10.1080/10426507.2024.2427148

To link to this article: https://doi.org/10.1080/10426507.2024.2427148

PHOSPHORUS, SULFUR, AND SILICON AND THE RELATED ELEMENTS
2024, VOL. 199, NOS. 10–12, 864–875
https://doi.org/10.1080/10426507.2024.2427148

New 2-hydrazinothiazole derivatives as potential MAO-A, MAO-B, AChE, and BChE inhibitors

Beyzanur Tutuş[a,b,c], Asaf Evrim Evren[a,d,e], Begüm Nurpelin Sağlik Özkan[a], and Leyla Yurttaş[a]

[a]Department of Pharmaceutical Chemistry, Faculty of Pharmacy, Anadolu University, Eskişehir, Turkey; [b]Kırıkhan Vocational School, Hatay Mustafa Kemal University, Hatay, Turkey; [c]Institute of Graduate Education, Anadolu University, Eskişehir, Turkey; [d]Vocational School of Health Services, Bilecik Şeyh Edebali University University, Bilecik, Turkey; [e]Department of Analytical Chemistry, Faculty of Pharmacy, Anadolu University, Eskişehir, Turkey

ABSTRACT

The incidence of neurodegenerative Alzheimer's and Parkinson's diseases is increasing worldwide every day, and treatment options are currently very limited. There is no definitive cure for these diseases, and the drugs available in clinical practice only provide symptomatic relief without halting the progression of neurodegeneration. One commonly employed strategy in the treatment of Alzheimer's and Parkinson's diseases is to return neurotransmitter levels by inhibiting enzymes like cholinesterase (ChE) and monoamine oxidase (MAO). In this research, we focused on investigating the therapeutic potential of 2-[2-(substituted benzylidene)hydrazinyl]-4-(substituted phenyl)thiazole derivatives (**2a**–**2h**) by incorporating hydrazine, known for its inhibitory effects on monoamine oxidases, into the structure of molecules that inhibit acetylcholinesterase. Thiazole ring was included in these derivatives due to its reported inhibitory activity against both cholinesterases and monoamine oxidase enzymes. When the enzyme inhibition activities were evaluated, it was determined that compounds **2c**, **2d**, and **2h** showed the highest inhibitory activity against AChE, while compounds **2f** and **2h** expressed the highest activity against MAO-B. It was determined that compound **2h** had the highest inhibitory activity on both AChE ($0.030 \pm 0.001\ \mu$M) and MAO-B ($0.048 \pm 0.002\ \mu$M) and compound **2h** was the only compound with conspicuous dual inhibitory activity. Furthermore, molecular docking calculations and molecular dynamics simulations were found to agree with experimental results.

ARTICLE HISTORY
Received 21 May 2024
Accepted 31 October 2024

KEYWORDS
2-Hydrazinothiazole; acetylcholinesterase inhibition; monoamine oxidase inhibition; molecular dynamic simulation

GRAPHICAL ABSTRACT

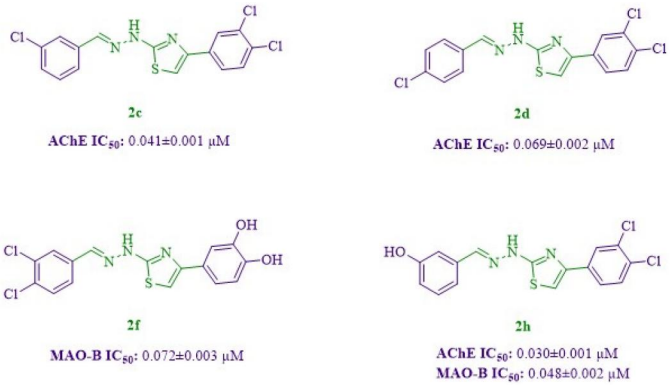

Introduction

Cholinesterases (ChEs) are part of the serine hydrolase enzyme family and are encoded by two separate genes, specifically acetylcholinesterase (AChE) and butyrylcholinesterase (BChE). These enzymes have important functions in controlling cholinergic signaling and ensuring the optimal operation of the nervous system [1,2]. In the cholinergic pathway, which includes acetylcholine in both the central and peripheral nervous systems, AChE plays an important role in the degradation of acetylcholine. Conversely, BChE is tasked with breaking down various choline esters, which include acetylcholine. AChE and BChE display significant distinctions in their selectivity for various substrates, their enzymatic speed, their activity levels, and their localization in specific brain regions. These disparities are instrumental in defining their distinct functions and how they are controlled in the processes of cholinergic neurotransmission [3–5]. Monoamine oxidase (MAO) is an enzyme primarily situated

CONTACT Beyzanur Tutuş beyzanurtutus@anadolu.edu.tr; beyzanur.tutus@mku.edu.tr Department of Pharmaceutical Chemistry, Faculty of Pharmacy, Anadolu University, Eskişehir, Turkey

Supplemental data for this article can be accessed online at https://doi.org/10.1080/10426507.2024.2427148.

in the outer mitochondrial membrane of both neuronal and non-neuronal cells. Its primary role revolves around the oxidative deamination of endogenous monoamines, which encompass noradrenaline, adrenaline, dopamine, serotonin, and tyramine. In the human system, two distinct forms of MAO enzymes exist, known as MAO-A and MAO-B. These enzymes serve vital functions in controlling amine metabolism, neurotransmitter levels, and the storage of intracellular amines [6–8]. Monoamine oxidase inhibitors (MAOIs) are employed to prevent the deamination or breakdown of neurotransmitters. They find frequent use in the treatment of depressive disorders, Parkinson's disease, anxiety disorders, and Alzheimer's disease. By inhibiting the activity of MAO, MAOIs elevate the levels of monoamine neurotransmitters in the brain, thereby alleviating symptoms associated with these conditions [7,9]. MAOIs also play an important role in therapeutic effects such as neuroprotection and neurological rescue, which are effective in the treatment of Alzheimer's disease (AD) [10].

AD is a chronic neurodegenerative condition associated with the aging process. It is marked by substantial cognitive function impairment, memory loss, and a gradual deterioration in daily activities. Additionally, symptoms encompass behavioral challenges such as anxiety, depression, and severe memory loss [11–13]. AD's global prevalence is on the rise, with nearly 50 million individuals currently afflicted, and this figure is projected to triple by the year 2050. In Europe, it is anticipated that the number of dementia patients will double by 2050 [14].

It has been confirmed that individuals with AD possess a cholinergic system in their brains, and it's noticeable that this system's activity diminishes postmortem. The decline in cognitive function in AD is linked to reduced levels of ACh within the brain. This understanding has prompted research into cholinergic medications through clinical trials. Inhibiting the enzymes AChE and BChE holds promise for elevating ACh levels in the brain. Consequently, AChE/BChE inhibitors have received approval for addressing the symptomatic aspects of AD [11,15,16].

Parkinson's Disease (PD) is a progressive neurological disorder characterized by the specific loss of dopaminergic neurons in the substantia nigra pars compacta [17].

The treatment of PD primarily focuses on enhancing dopaminergic levels and addressing complications. This involves drugs like L-dopa, dopamine agonists, MAO-B inhibitors, and COMT inhibitors for the dopaminergic system, alongside non-dopaminergic drugs like anticholinergics. These treatments aim to optimize dopamine function and alleviate symptoms.

Both AD and PD involve cholinergic and dopaminergic system dysfunction, leading to drug development strategies centered on restoring neurotransmitter levels by inhibiting ChE and MAO enzymes [18]. Because Alzheimer's disease has a complex pathophysiology, medications used to treat Alzheimer's may not be an effective strategy. Therefore, many research groups have focused on developing multi-target agents (MTAs) for effective drug candidates in the treatment of Alzheimer's disease. The design strategy of MTAs is to include pharmacophoric groups of different drugs in the same structure. Therefore, it is thought that a ligand with MAO inhibitor potential may have a more effective therapeutic effect in AD if it also has AChE inhibitor activity. This is why there are many studies on the development of MTA [19–21].

Thiazole derivatives are known to have various pharmacological effects, such as antimicrobial [22] antimalarial [23], antitubercular [24], antiviral [25], anti-inflammatory [26], antidiabetic [27], anticonvulsant [28], antioxidant [29], anticancer [30] and cardiovascular activity [31]. Furthermore, there are studies on the monoamine oxidase inhibitor and cholinesterase inhibitor activity of 2-hydrazinothiazole derivatives [32–40]. In addition, in previous studies, it was determined that the 4-arylthiazol-2-yl-hydrazine structure was a pharmacophore group for MAO inhibition activity [36].

Building upon the information mentioned earlier, our research involves the synthesis of derivatives of 2-[2-(substituted benzylidene)hydrazinyl]-4-(substituted phenyl)thiazoles (**2a–2h**). Considering the promising characteristics and effects typically associated with compounds featuring the thiazole ring, we anticipate that these newly synthesized compounds could serve as promising candidates for addressing AD and PD. However, to gauge their effectiveness and suitability for therapeutic purposes in these diseases, further investigations and evaluations are necessary.

A series of 2-hydrazinothiazole derivatives have been synthesized in the studies reported in the literature [36,41,42] and the most active compounds of the series when evaluated for MAO activities are shown in Figure 1. Furthermore, in one of the studies reported [38], 2-hydrazinothiazole derivatives were synthesized and evaluated for MAO and AChE activities and the most active compounds of serine dual inhibitors against MAO-B and AChE are shown in Figure 1 [36,38,41,42]. In light of all this information, new 2-hydrazinothiazole derivatives were synthesized and MAOI and ChEI activities were investigated in this study.

Results and discussion

Chemistry

In the first step, benzaldehyde derivatives were reacted with thiosemicarbazide, resulting in the formation of thiosemicarbazones (**1a-1f**). In the second step, the 2-(substituted benzylidene)hydrazinecarbothioamide derivatives obtained from the first step were reacted with 2-bromo-3',4'-(disubstituted acetophenone) derivatives according to Hantzsch thiazole synthesis, leading to the final compounds showed **Figure 2** (**2a-2h**).

The structures of the synthesized 2-[2-(substituted benzylidene)hydrazinyl]-4-(substituted phenyl)thiazole derivatives were checked by ^{1}H and ^{13}C NMR spectroscopy and mass spectrometry.

The IR spectra of 2-[2-(substituted benzylidene)hydrazinyl]-4-(substituted phenyl)thiazoles **2a–2h** were investigated. The bands of the N-H bond stretching in all compounds and the O-H bond stretching in some compounds were found to be between 3325 and 3070 cm^{-1}.

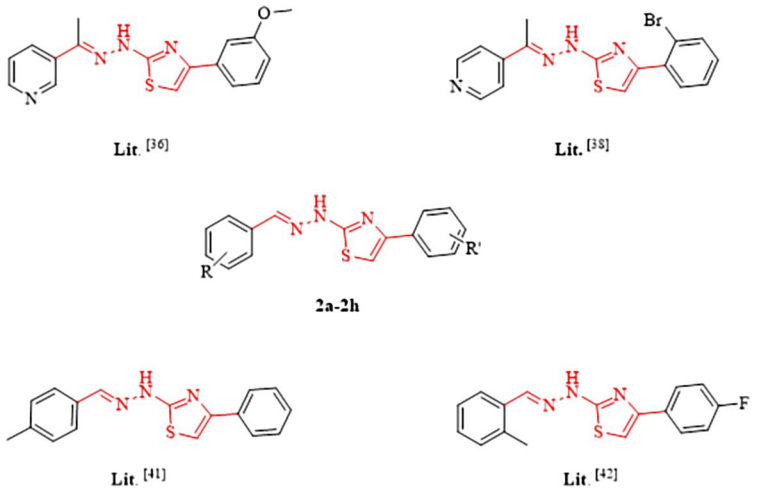

Figure 1. 2-Hydrazinothiazole framework in some studies and **2a**–**2h** compounds.

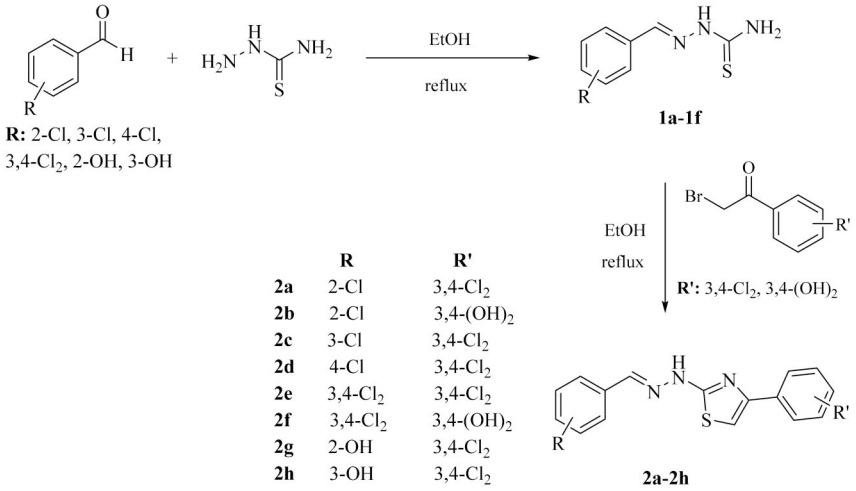

	R	R'
2a	2-Cl	3,4-Cl_2
2b	2-Cl	3,4-$(OH)_2$
2c	3-Cl	3,4-Cl_2
2d	4-Cl	3,4-Cl_2
2e	3,4-Cl_2	3,4-Cl_2
2f	3,4-Cl_2	3,4-$(OH)_2$
2g	2-OH	3,4-Cl_2
2h	3-OH	3,4-Cl_2

Figure 2. Synthesis of 2-[2-(substituted benzylidene)hydrazinyl]-4-(substituted phenyl)thiazoles **2a**–**2h**.

In addition, it was observed that the bands for aromatic C-H stretching were between 3159 and 3043 cm^{-1}, the bands for aliphatic C-H stretching were between 2941 and 2791 cm^{-1} and the bands for C = C and C = N stretching were between 1624 and 1386 cm^{-1}. When the compounds containing 1,2-disubstituted, 1,3-disubstituted, 1,4-disubstituted, and 1,3,4-trisubstituted benzene rings were examined, it was determined that the out-of-plane deformation bands of these parts were between 962 and 723 cm^{-1}.

^{1}H-NMR spectra of the synthesized compounds were recorded at 300 MHz. The signals of the synthesized compounds were observed in the range of 6.76–12.73 ppm. The signal belonging to the amino group in the compounds was observed only in the derivatives containing the chloro substituent and these signals were found to be in the range of 12.17–12.73 ppm as singlet. In compounds containing the hydroxyl group, the signal belonging to this group was observed to be in the range of 9.62–10.09 ppm. The signals for the aromatic protons are in the range of 6.76–8.33 ppm in all compounds.

According to the ^{13}C NMR spectra of the synthesized final compounds, the signal of the carbon atom in the second position of the thiazole ring appears in the range of 168.8–168.0 ppm, while the signal of the carbon atom in the fourth position is in the range of 145.9–150.2 ppm. The signal of azomethine carbon atom in all compounds was detected in the range of 138.0–146.0 ppm. The NMR signal of the carbon atom, to which the hydroxyl group is attached, is observed at around 158.0 ppm, while the NMR signals of the other carbon atoms are observed in the region up to 106.6 ppm.

The compounds, of which the mass spectra were recorded, showed a peak compatible with the $M+1$ ion. In addition, the molecular weight of the compound, the mass spectrum of which was obtained by the APCI-MS method, is compatible with the M + H peak observed.

Evaluation of physicochemical parameters of synthesized compounds

In order for a molecule to be effective as a drug, it must reach its target in the body in sufficient concentration and remain in a bioactive form for a sufficient time for the expected biological events to occur there [43]. Determination of these properties is included in the activity assessment and *in vivo* pharmacokinetic studies for active compounds may be

considered in the following studies. For this reason, the medicinal chemistry and pharmacokinetic profiles of the designed compounds were calculated with the Swiss-ADME web-based program.

In silico ADME (Absorption, Distribution, Metabolization, and Elimination) study was performed for the synthesized 2-[2-(substituted benzylidene)hydrazinyl]-4-(substituted phenyl)thiazole derivatives **2a**–**2h** (Table 1). The number of hydrogen bond acceptor atoms (HBA), hydrogen bond donors (HBD), topological polar surface area (TPSA), partition coefficient (Log P), water solubility (Log S), skin permeability coefficient (Log Kp), and gastrointestinal absorption (GI Abs.) were determined and were scored according to 5 different filters in terms of drug-likeness. It has been determined that the molecular weight is in the range of 345.80–417.14, the number of hydrogen bond acceptor atoms is the range of 2–4, the number of hydrogen bond donor atoms is the range of 1–3, the topological polar surface area is the range of 65.52–105.98, and the log P is the range of 3.51–5.86. In addition, it was determined that the compounds have a high absorption rate in the GI tract whereas moderate rate in the skin [44].

When the drug likeness of the synthesized compounds was examined according to the Lipinski, Veber, Ghose, Muegge, and Egan rules, it was seen that the compounds passed 2, 4, and 5 of them. According to the rules set by Lipinski et al., the physicochemical ranges required for the compounds to have a high probability of being an oral drug were determined [43]. Based on the evaluation of Lipinski's five drug-likeness rule, all the compounds synthesized in this study were found to meet the criteria, indicating their suitability as potential oral drugs in terms of key parameters.

Evaluation of enzyme inhibition activity

In this study, the inhibitory activities of the synthesized 2-[2-(substituted benzylidene)hydrazinyl]-4-(substituted phenyl)thiazole derivatives **2a**–**2h** on AChE, BChE, MAO-A, and MAO-B enzymes were investigated (Table 2). All enzymes were studied at 10^{-3} and 10^{-4} M concentrations and the results were expressed as percent inhibition. Donepezil was used as a reference drug for AChE inhibition and tacrine for BChE inhibition, moclobemide for MAO-A inhibition and selegiline for MAO-B inhibition.

Table 1. Physicochemical properties of compounds **2a**–**h**.

	MW	HBA	HBD	TPSA	Log P	GI Abs.	BBB	Log K_p	DL
2a	382.69	2	1	65.52	5.36	High	No	−4.05	2/5
2b	345.80	4	3	105.98	3.51	High	No	−5.23	5/5
2c	382.69	2	1	65.52	5.35	High	No	−4.05	2/5
2d	382.69	2	1	65.52	5.34	High	No	−4.05	2/5
2e	417.14	2	1	65.52	5.86	High	No	−3.82	2/5
2f	380.25	4	3	105.98	4.02	High	No	−4.99	4/5
2 g	364.25	3	2	85.75	4.42	High	No	−4.64	4/5
2h	364.25	3	2	85.75	4.40	High	No	−4.64	4/5

MW: Molecular weight; HBA: Hydrogen bond acceptor; HBD: Hydrogen bond donors; TPSA: Topological polar surface area (Å^2); Log P: Partition coefficient; GI Abs: Gastrointestinal absorption; BBB: Blood-brain barrier; Log Kp: Skin permeability coefficient; DL: Druglikeness. Calculations were made *via* http://www.swissadme.ch/index.php#.

Table 2. Synthesized compounds IC_{50} (μM) values and % inhibition rates against AChE, BChE, MAO-A, and MAO-B enzymes at 10-3 and 10-4 M concentrations.

	AChE % Inhibition			BChE % Inhibition			MAO-A % Inhibition			MAO-B % Inhibition		
Compounds	10^{-3} M	10^{-4} M	AChE IC_{50} (μM)	10^{-3} M	10^{-4} M	BChE IC_{50} (μM)	10^{-3} M	10^{-4} M	MAO-A IC_{50} (μM)	10^{-3} M	10^{-4} M	MAO-B IC_{50} (μM)
2a	70.821 ± 1.839	39.016 ± 0.782	>100	31.413 ± 0.923	26.921 ± 0.875	>1000	42.460 ± 0.932	34.002 ± 0.855	>1000	52.913 ± 1.351	26.861 ± 0.822	>100
2b	68.635 ± 1.351	41.379 ± 0.956	>100	28.664 ± 0.731	20.346 ± 0.974	>1000	29.618 ± 0.737	21.236 ± 0.651	>1000	48.464 ± 0.748	31.602 ± 0.936	>1000
2c	94.667 ± 1.869	89.529 ± 1.130	0.041 ± 0.001	26.859 ± 0.890	21.235 ± 0.757	>1000	36.567 ± 1.030	30.642 ± 1.047	>1000	61.682 ± 1.136	30.448 ± 0.929	>100
2d	92.055 ± 2.036	86.681 ± 0.997	0.069 ± 0.002	34.018 ± 0.828	30.059 ± 0.905	>1000	41.028 ± 0.830	31.851 ± 0.957	>1000	40.091 ± 0.702	27.671 ± 0.977	>1000
2e	48.552 ± 0.899	37.940 ± 0.667	>1000	29.197 ± 0.977	23.400 ± 0.790	>1000	39.711 ± 0.996	33.929 ± 0.613	>1000	39.358 ± 0.755	30.426 ± 0.913	>1000
2f	68.018 ± 1.056	34.757 ± 0.790	>100	37.452 ± 0.836	24.764 ± 0.857	>1000	29.620 ± 0.847	22.034 ± 0.708	>1000	92.064 ± 2.147	89.150 ± 1.699	0.072 ± 0.003
2g	82.110 ± 1.662	48.490 ± 1.057	>100	36.610 ± 1.146	27.850 ± 0.922	>1000	39.330 ± 1.163	31.928 ± 0.947	>1000	70.733 ± 1.656	43.130 ± 0.971	>100
2h	96.267 ± 2.133	91.308 ± 1.840	0.030 ± 0.001	28.362 ± 0.851	20.609 ± 0.830	>1000	42.489 ± 0.848	30.348 ± 0.674	>1000	94.485 ± 2.108	91.227 ± 1.566	0.048 ± 0.002
Donepezil	99.156 ± 1.302	97.395 ± 1.255	0.0201 ± 0.0010	–	–	–	–	–	–	–	–	–
Tacrine	–	–	–	99.827 ± 1.378	98.651 ± 1.402	0.0064 ± 0.0002	–	–	–	–	–	–
Moclobemide	–	–	–	–	–	–	94.121 ± 2.760	82.143 ± 2.691	6.0613 ± 0.2625	–	–	–
Selegiline	–	–	–	–	–	–	–	–	–	98.589 ± 2.055	94.850 ± 1.114	0.0374 ± 0.0016

AChE inhibition activity

The AChE percent inhibition values of the compounds were found to be between 48.552 ± 0.899% and 96.267 ± 2.133% for 10^{-3} M concentration and, between 34.757 ± 0.790% and 91.308 ± 1.840% when evaluated for the 10^{-4} M concentration. For donepezil, the reference drug for AChE inhibition, these values were 99.156 ± 1.302% at 10^{-3} M concentrations, and 97.395 ± 1.255% at 10^{-4} M concentrations. The compounds **2c** (IC_{50}: 0.041 ± 0.001 μM), **2d** (IC_{50}: 0.069 ± 0.002 μM), and **2h** (IC_{50}: 0.030 ± 0.001 μM) showed significant AChE inhibition whereas the reference drug donepezil has an IC_{50} value of 0.0201 ± 0.0010 μM. The IC_{50} values of the other compounds could not be calculated.

BChE inhibition activity

BChE percent inhibition values of the compounds were found between 26.589 ± 0.890% and 37.452 ± 0.836% for the 10^{-3} M concentration and between 20.346 ± 0.974 and 30.059 ± 0.905% for the 10^{-4} M concentration. These values were 99.827 ± 1.378% at the 10^{-3} M concentration and 98.651 ± 1.402% at the 10^{-4} M concentration for tacrine, the reference drug for BChE inhibition. IC_{50} values of the compounds could not be calculated as none of the compounds showed 50% inhibition.

MAO-A inhibition activity

The MAO-A percent inhibition values of the compounds were found to be between 29.618 ± 0.737% and 42.489 ± 0.848% when evaluated for 10^{-3} M concentration, and between 21.236 ± 0.651% and 34.002 ± 0.855% when evaluated for 10^{-4} M concentration. For moclobemide, the reference drug for MAO-A inhibition, these values were 94.121 ± 2.760% at the 10^{-3} M concentration and 82.143 ± 2.691% at the 10^{-4} M concentration. The IC_{50} values of the compounds could not be calculated as none of the compounds showed 50% or greater inhibition.

MAO-B inhibition activity

The percent inhibition values of MAO-B of the compounds were found to be between 39.358 ± 0.755 and 94.485 ± 2.18% for the 10^{-3} M concentration, and between 26.861 ± 0.822 and 91.227 ± 1.566% when evaluated for the 10^{-4} M concentration. For selegiline, the reference drug for MAO-B inhibition, these values are 98.589 ± 2.055% at the 10^{-3} M concentration and 94.850 ± 1.14% at the 10^{-4} M concentration. The IC_{50} value of most of the compounds could not be calculated. However, IC_{50} values of **2f** (0.072 ± 0.003 μM) and **2h** (0.048 ± 0.002 μM) compounds were calculated. The IC_{50} value of the reference drug selegiline is 0.0374 ± 0.0016 μM.

Evaluation of molecular Docking studies

Docking study on MAO-B enzyme

According to the *in vitro* MAO-B inhibition results, it was determined that the synthesized substances showed activity on the target proteins. To understand the structure-activity relationship with the obtained inferences, placement studies were carried out (Figure 3). The binding forms of the active compounds **2f** and **2h** on MAO-B are given in Table 3. According to these interactions, all of the compounds interacted with the FAD (Flavin adenine dinucleotide) protein. This interaction of the compounds has been observed as hydrogen bonding. In addition, the interaction of tyrosine amino acids (seq. 398 and 435) with FAD is essential for enzyme activity, thus, interactions with these enzymes play a key role in inhibition activity. However, it is known that binding of the ligand with amino acids Ile199 and Gln202 contributes to the inhibition activity [33]. For this reason, it can be said that in the interactions of the **2f** and **2h** with the FAD protein the interactions with these amino acids are especially effective. In conclusion, the interaction of compound **2h** with both FAD protein and important pocket amino acids is in agreement with the results from *in vitro* tests. Basically, the two-site chlorine substitution of the phenyl ring on the thiazole moiety allowed this end of the molecule to remain at the protein's pocket entrance, while the hydroxy substituent at the other end formed a hydrogen bond with the FAD protein.

Docking study on AChE enzyme

According to the results obtained from *in vitro* AChE enzyme inhibition tests, active compounds were determined and a molecular docking study was carried out in order to examine the structure-effect relationships at the molecular level. The best 2D and 3D poses of the compounds are shown in Figure 4. The way the compounds bind to the AChE enzyme and their binding numbers are indexed in Table 4. Docking results showed π-π interaction with Trp86 amino acid for all compounds. In addition, it was determined that all compounds, except for compound **2c**, bind to the amino acid Trp286. Trp86 and Trp286, designated as catalytic active site (CAS) amino acid and peripheral anionic site (PAS) amino acid, respectively, are important in enzyme activity and enzyme inhibition activity [45]. Therefore, most probably these interactions are the basis of the activity of these compounds. Moreover, the placement of compound **2c** in the acyl pocket, which is an important pocket that facilitates the hydrolysis of acetylcholine, and the hydrogen bond formation there with Phe295, may have stabilized the ligand-enzyme complex and thus exerted its inhibition effect. In all, the results of the enzyme activity of the compounds and the results of the docking study were found to be in agreement. In terms of structure-effect relationship, the binding of the monosubstituted phenyl ring with Trp86 from the 3rd or 4th position attached to the hydrazone moiety was found to be important for the activity.

Evaluation of molecular dynamic simulation (MDS) studies

The stability of the model compound **2h** was evaluated through a molecular dynamics simulation (MDS) study to understand its interactions and behavior under environmental

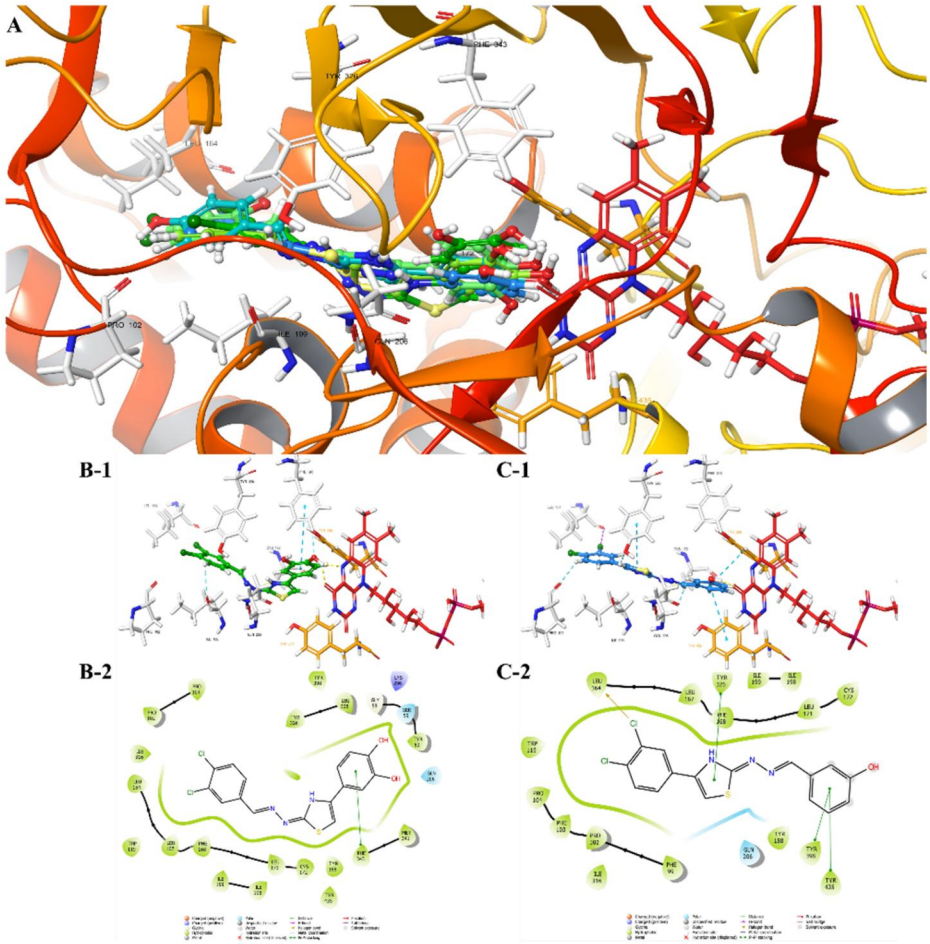

Figure 3. The best 2D and 3D representation of active compounds in the MAO-B active pocket. (A) 3D exposure of superimposed active compounds. (B-1, B-2) 3D and 2D representation of compound **2f** in the active pocket. (C-1, C-2) 3D and 2D representation of compound **2h** in the active pocket.

Table 3. Interaction index of MAO-B enzyme and active compounds.

Compounds	Enzyme part	Type and number of bond
2f	• Ile199	• 1 Ar H-bond
	• Phe343	• 1 π-π interaction
	• Phe343	• 1 Ar H-interaction
	• FAD	• H-bond
	• FAD	• H-bond
2h	• Pro102	• 1 Ar H-bond
	• Leu164	• 1 halogen bond
	• Tyr326	• 1 π-π interaction
	• Tyr326	• 1 Ar H-bond
	• Gln206	• 1 Ar H-bond
	• Tyr398	• 1 π-π interaction
	• Tyr435	• 1 π-π interaction
	• FAD	• 1 H-bond

changes. The RMSD value is used to analyze the stability of the protein-ligand complex during the simulation time (as shown in Figure 5A–C) [46]. The protein RMSD is in the acceptable range of 1–3 Å [47].

The RMSF value offers a stability diagram of the rigid and flexible regions of the protein structure [48,49]. For the stability of the proteins in the RMSF graphs, the fluctuation should be similar or less when considering the form of the protein [50]. The RMSF plot indicated that the peaks of interacted residues with the loop region were observed under 1 Å similar to α-helices (red areas) and β-strands (blue areas).

The residues Asp74, Gly122, Ser203, and Trp286 were determined to be continuously interacting with compound **2h** (as shown in Figure 5D). Hydrophobic interactions were observed with Trp86, Trp286, Phe297, Tyr337, Phe338, Tyr341, and His447 while the water-mediated H-bonds were found with Asp74, Asn87, Tyr124, Tyr337, and Tyr341 (as shown in Figure 5D,E). Additionally, there were some direct H-bonds with Asp74, Gly122, Tyr124, Ser203, Tyr337, and His447. Meanwhile, compound **2h** also interacted with various amino acids *via* π-π stacking, aromatic H-bonds, and halogen bonds. The π-π stackings were observed between ligand and Trp286, Tyr337, Phe338, and Tyr341; aromatic H-bonds were observed with Asp74, Ser203, Trp286, Tyr337, Tyr341, and His447 and halogen bonds were observed with Tyr72. The most stable interactions were with Asp74, Trp86, Gly122, Tyr124, Ser203, Trp286, Tyr337, Phe338, and Tyr341 and are shown in Figure 5F and in a video (see Supplemental Materials). In the video of the molecular dynamics simulation, all interactions between **2h** and the AChE enzyme during the entire simulation time can be viewed.

Conclusions

The 2-[2-(substituted benzylidene)hydrazinyl]-4-(substituted phenyl)thiazoles **2a**–**2h** were synthesized in two steps. The structures of the synthesized compounds were confirmed by ^{1}H NMR,^{13}C NMR, IR spectroscopy and mass spectrometry.

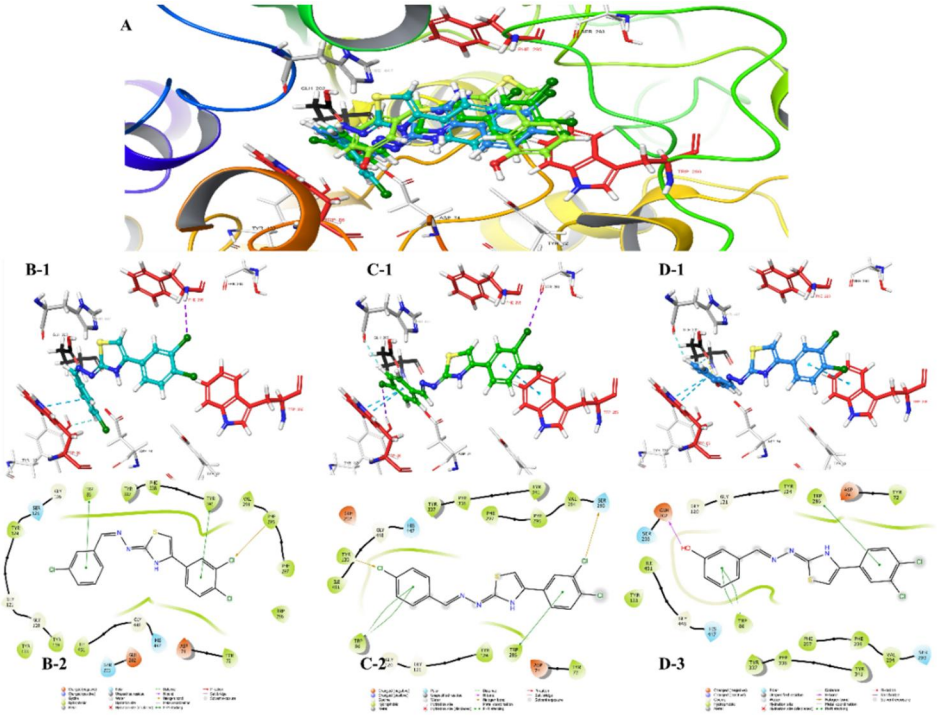

Figure 4. The best 2D and 3D representation of active compounds in the AChE active pocket. (A) 3D exposure of superimposed active compounds. (B-1, B-2) 3D and 2D representation of compound compound **2c** in the active pocket. (C-1, C-2) position of compound **2d** in the active pocket. (D-1, D-2) 3D and 2D representation of compound **2h** in the active pocket.

Table 4. Interaction index of AChE enzyme and active compounds.

Compounds	Enzyme part	Type and number of bond
2c	• Trp86	• 1 π-π interaction
	• Tyr133	• 1 Ar H-bond
	• Phe295	• 1 halogen bond
	• Tyr341	• 1 π-π interaction
2d	• Trp86	• 2 π-π interactions
	• Tyr133	• 1 halogen bond
	• Trp286	• 1 π-π interaction
	• Ser293	• 1 halogen bond
	• His447	• 1 Ar-H-bond
2h	• Trp86	• 1 π-π interaction
	• Glh202	• 1 Ar H-bond
	• Glh202	• 1 H-bond
	• Trp286	• 1 π-π interaction
	• His447	• 1 Ar H-bond

The synthesized final compounds exhibited a higher inhibitory effect against AChE and MAO-B compared to their inhibitory effect against BChE and MAO-A.

Compounds **2c**, **2d**, and **2h** exhibited the highest activity against AChE, while compounds **2f** and **2h** showed the highest activity against MAO-B. Notably, compound **2h** demonstrated the highest inhibitory activity against both AChE ($0.030 \pm 0.001\ \mu$M) and MAO-B ($0.048 \pm 0.002\ \mu$M), making it the only compound with dual inhibitory activity. Although the compounds did not reach the activity level of the reference drugs donepezil and selegiline, they displayed activity that was very close to these references.

It has been revealed in many studies in the literature that compounds containing 2-hydrazinothiazole in their structure show MAO inhibition and anticholinesterase activity. Based on the extensive available information, our study found that the newly designed hydrazinothiazoles exhibited inhibitory effects on MAO and AChE enzymes. Notably, 2-[2-(3-hydroxybenzylidene)hydrazinyl]-4-(3,4-dichlorophenyl) thiazole **2h** displayed the highest activity against both enzymes. Moving forward, future studies are being contemplated to design compounds utilizing these structures, aiming to achieve dual inhibitory activity against AChE and MAO-B enzymes. The docking calculation and molecular dynamics simulation studies revealed importantly that the 3-hydroxy group increases the stability in the CAS region of AChE while 4-phenyl thiazole shows contacts with residues of the PAS region. Hence, these two moieties play an important role in AChE inhibition when combined with hydrazone pharmacophore core.

Materials and methods

Chemistry

All of the materials used in the synthesis of the compounds are from Sigma-Aldrich Pty. Ltd. (Germany) and Merck Pty. Ltd. (Germany). The NMR spectra of the synthesized compounds were recorded using a Bruker spectrometer operating at 300 MHz (^{1}H) and 75 MHz (^{13}C). IR spectra were measured using a Shimadzu-IR Affinity-IS instrument. Mass spectrum measurement was performed by Electrospray Ionization Mass Spectrometry (ESI) using an LCMS-IT-TOF device. In addition, the measurement of some of the mass spectra was carried out with an Advion Compact Mass Spectrometer, USA. The melting points of the compounds were determined using the Mettler Toledo-MP90 Melting Point System.

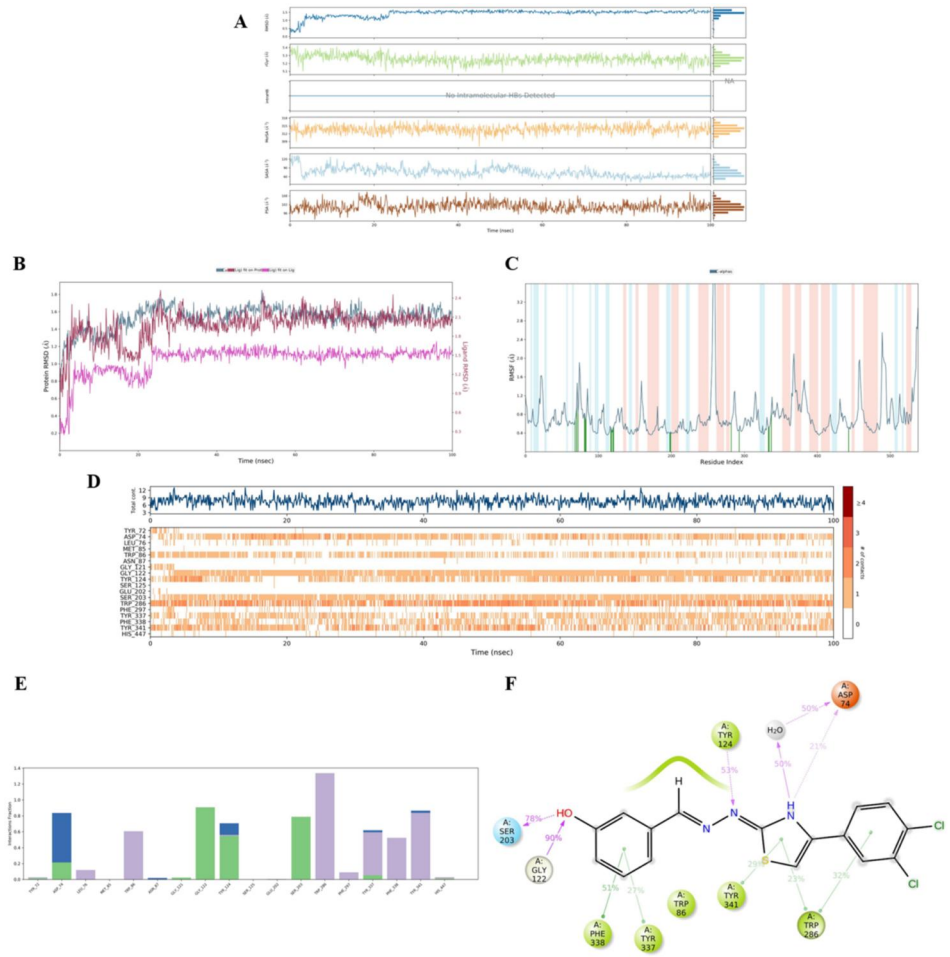

Figure 5. MDS results for **2h** and AChE protein complex. (A) Physicochemical properties of the ligand. (B) RMSD plot of the protein, the ligand versus protein, and the ligand versus ligand. (C) RMSF plot of the complex. (D) Number of interactions and interaction types versus time plot. (E) Plot of interaction fractions versus residues with their interaction types during the time. (F) 2D diagram for contact strength.

Synthesis of 2-(substituted benzylidene)hydrazinecarbothioamides 1a–f (method A)

For the synthesis of 2-(substituted benzylidene) hydrazinecarbothioamides **la**–**f**, a mixture of 11 mmol of the appropriate benzaldehyde derivative and 11 mmol of thiosemicarbazide was dissolved in about 30 mL of ethanol. This mixture was boiled at reflux for 6–8 h. The progress of the reaction was monitored by TLC. The precipitated product was then filtered and dried. It was recrystallized from ethanol.

Synthesis of 2-[2-(substituted benzylidene)hydrazinyl]-4-(substituted phenyl)thiazoles 2a–h (method B)

For the synthesis of 2-[2-(substituted benzylidene)hydrazinyl]-4-(substituted phenyl)thiazoles **2a**–**h**, 0.3 grams of each of the 2-(substituted benzylidene)hydrazinecarbothioamides **la**–**f** was taken separately and dissolved in ∼100 mL of alcohol. An equimolar quantity of the respective 2-bromoacetophenone derivative was added to the solution, followed by refluxing for a period of 24–36 h. The progress of the reaction was monitored using TLC. Upon completion, the resulting product was precipitated, filtered, and subsequently dried. Finally, the product was subjected to crystallization from ethanol.

2-[2-(2-Chlorobenzylidene)hydrazinyl]-4-(3,4-dichlorophenyl)thiazole (2a)

Yield 65%, m.p. 180–182 °C. IR (ATR): ν_{max} (cm^{-1}) = 3172 (N-H stretching band), 3159–3059 (aromatic C-H stretching band), 2910–2791 (aliphatic C-H stretching band), 1597–1573 (C = N and C = C stretching band), 931–725 (1,2-disubstituted benzene and 1,3,4-trisubstituted benzene out-of-plane bending bands).^{1}H NMR (300 MHz, DMSO-d_6): δ = 7.63–7.69 (m. 2H, Ar-H), 7.74–7.79 (m, 1H, Ar-H), 7.84–7.86 (m, 1H, Ar-H), 7.90–7.95 (m, 1H, Ar-H), 8.11 (dd, J = 8.0 Hz, 2.0 Hz, 1H, Ar-H), 8.16–8.21 (m, 1H, Ar-H), 8.34–8.35 (m, 1H, Ar-H), 8.66 (s, 1H, Ar-H), 12.73 (br s, 1H, N-H). ^{13}C NMR (75 MHz, DMSO-d_6): δ = 107.1, 126.3, 126.9, 127.9, 128.3, 130.5, 131.4, 131.6, 133.0, 135.8, 138.0, 148.8, 168.8. HRMS (m/z): $[M+H]^+$: Calcd. for $C_{16}H_{10}C_3N_3S$: 381.9750, found: 381.9734.

2-[2-(2-Chlorobenzylidene)hydrazinyl]-4-(3,4-dihydroxyphenyl)thiazole (2b)

Yield 68%, m.p. 201–204 °C. IR (ATR): ν_{max} (cm^{-1}) = 3325–3211 (O-H and N-H stretching band), 3072 (aromatic C-H stretching band), 1624–1525 (C = N and C = C stretching band), 823–761 (1,2-disubstituted and 1,3,4-trisubstituted benzene out-of-plane bending bands). ^{1}H NMR

(300 MHz, DMSO-d_6): $\delta = 6.78$ (d, $J = 8.2$ Hz, 1H, Ar-H), 7.02 (s, 1H, Ar-H), 7.12 (dd, $J = 8.2$ Hz, 2.2 Hz, 1H, Ar-H), 7.25 (d, $J = 2.2$ Hz, 1H, Ar-H), 7.39–7.43 (m, 2H, Ar-H), 7.49–7.52 (m, 1H, Ar-H), 7.92–7.95 (m, 1H, Ar-H), 8.47 (br s, 1H, Ar-H). ^{13}C NMR (75 MHz, DMSO-d_6): $\delta = 101.7$, 113.9, 116.2, 117.6, 126.0, 126.8, 128.1, 130.4, 131.2, 132.0, 132.8, 138.3, 145.7, 146.0, 150.2, 168.1. HRMS (m/z): $[M + H]^+$: Calcd. for $C_{16}H_{12}ClN_3O_2S$: 346.0412, found: 346.0414.

2-[2-(3-Chlorobenzylidene)hydrazinyl]-4-(3,4-dichlorophenyl)thiazole (2c)

Yield 72%, m.p. 186–187 °C. IR (ATR): ν_{max} (cm^{-1}) = 3113 (N-H stretching band), 3062 (aromatic C-H stretching band), 2848 (aliphatic C-H stretching band) 1558–1386 (C = N and C = C stretching band), 927–731 (1,3-disubstituted and 1,3,4 trisubstituted benzene out-of-plane bending bands). ^{1}H NMR (300 MHz, DMSO-d_6): $\delta = 7.44$–7.49 (m, 2H, Ar-H), 7.58–7.69 (m, 4H, Ar-H), 7.84 (d, $J = 8.5$ Hz, 1H, Ar-H), 8.02 (s, 1H, Ar-H), 8.08 (s, 1H, Ar-H), 12.37 (s, 1H, N-H). ^{13}C NMR (75 MHz, DMSO-d_6): $\delta = 106.7$, 125.4, 126.0, 127.6, 127.6, 129.4, 130.2, 131.2, 131.3, 131.9, 134.1, 135.6, 137.0, 140.3, 148.5, 168.7. HRMS (m/z): $[M + H]^+$: Calcd. for $C_{16}H_{10}Cl_3N_3S$: 381.9734, found: 381.9751.

2-[2-(4-Chlorobenzylidene)hydrazinyl]-4-(3,4-dichlorophenyl)thiazole (2d)

Yield 64%, m.p. 202–203 °C. IR (ATR): ν_{max} (cm^{-1}) = 3122 (N-H stretching band), 3049 (aromatic C-H stretching band), 2941–2796 (aliphatic C-H stretching band), 1595–1552 (C = N and C = C stretching band), 929–727 (1,4-disubstituted and 1,3,4 trisubstituted benzene out-of-plane bending bands). ^{1}H NMR (300 MHz, DMSO-d_6): $\delta = 7.50$ (d, $J = 8.6$ Hz, 2H, Ar-H), 7.58 (s, 1H, Ar-H), 7.66–7.70 (m, 3H, Ar-H), 7.84 (dd, $J = 8.4$ Hz, 2.0 Hz, 1H, Ar-H), 8.03 (s, 1H, Ar-H), 8.08 (d, $J = 2.0$ Hz, 1H, Ar-H), 12.32 (br s, 1H, N-H). ^{13}C NMR (75 MHz, DMSO-d_6): $\delta = 106.6$, 126.0, 127.6, 128.4, 129.4, 130.2, 131.4, 131.9, 133.7, 134.2, 135.6, 140.7, 148.5, 168.8. HRMS (m/z): $[M + H]^+$: Calcd. for $C_{16}H_{10}Cl_3N_3S$: 381.9734, found: 381.9722.

2-[2-(3,4-Dichlorobenzylidene)hydrazinyl]-4-(3,4-dichlorophenyl)thiazole (2e)

Yield 71%, m.p. 232–235 °C. IR (ATR): ν_{max} (cm^{-1}) = 3113 (N-H stretching band), 3128–3061 (aromatic C-H stretching band), 2929–2854 (aliphatic C-H stretching band), 1556–1473 (C = N and C = C stretching band), 925–723 (1,3,4-trisubstituted benzene out-of-plane bending bands). ^{1}H NMR (300 MHz, DMSO-d_6): $\delta = 7.58$ (s, 1H, Ar-H), 7.62–7.69 (m, 3H, Ar-H), 7.83 (dd, $J = 8.6$ Hz, 2.0 Hz, 1H, Ar-H), 7.86 (d, $J = 1.6$ Hz, 1H, Ar-H), 8.00 (s, 1H, Ar-H), 8.07 (d, $J = 2.0$ Hz, 1H, Ar-H), 12.42 (br s, 1H, N-H). ^{13}C NMR (75 MHz, DMSO-d_6): $\delta = 106.8$, 126.0, 126.4, 127.6, 128.2, 130.2, 131.3, 131.5, 131.8, 131.9, 132.1, 135.5, 135.6, 139.2, 148.5, 168.6. APCI-MS (-m/z): $[M + H]^+$: Calcd. for $C_{16}H_9Cl_4N_3S$: 417.13, found: 418.4.

2-[2-(3,4-Dichlorobenzylidene)hydrazinyl]-4-(3,4-dihydroxyphenyl)thiazole (2f)

Yield 69%, m.p. 209–210 °C. IR (ATR): ν_{max} (cm^{-1}) = 3197–3109 (O-H and N-H stretching band), 2916–2848 (aliphatic C-H stretching band), 1620–1516 (C = N and C = C stretching band), 962–783 (1,3,4-trisubstituted benzene out-of-plane bending bands). ^{1}H NMR (300 MHz, DMSO-d_6): $\delta = 6.76$ (d, $J = 8.2$ Hz, 1H, benzene 5-H), 7.00 (s, 1H, thiazole 5-H), 7.12 (dd, $J = 8.1$ Hz, 2.0 Hz, 1H, benzene 6-H), 7.24 (s, 1H, benzene 2-H), 7.63–7.71 (m, 2H, benzene 5-H and 6-H), 7.87 (d, $J = 1.4$ Hz, 1H, benzene 2-H), 8.03 (s, 1H, CH=N). ^{13}C NMR (75 MHz, DMSO-d_6): $\delta = 101.5$, 113.9, 116.1, 117.6, 126.5, 128.2, 131.5, 131.7, 132.1, 135.7, 139.2, 145.7, 145.9, 168.0. HRMS (m/z): $[M + H]^+$: Calcd. for $C_{16}H_{11}Cl_2N_3O_2S$: 380.0022, found: 380.0033.

2-[2-(2-Hydroxybenzylidene)hydrazinyl]-4-(3,4-dichlorophenyl)thiazole (2 g)

Yield 64%, m.p. 205–208 °C, Lit. m.p. 226.9–228 °C [51]. IR (ATR): ν_{max} (cm^{-1}) = 3140–3109 (O-H and N-H stretching band), 3043 (aromatic C-H stretching band), 2939–2791 (aliphatic C-H stretching band), 1606–1556 (C = N and C = C stretching band), 952–732 (1,2-disubstituted and 1,3,4-trisubstituted benzene out-of-plane bending bands). ^{1}H NMR (300 MHz, DMSO-d_6): $\delta = 7.85$–7.91 (m, 2H, Ar-H), 7.22 (t, $J = 7.8$ Hz, 1H, Ar-H), 7.55 (s, 1H, Ar-H), 7.63–7.68 (m, 2H, Ar-H), 7.84 (dd, $J = 8.4$ Hz, 1.9 Hz, 1H, Ar-H), 8.1 (d, $J = 2.1$ Hz, 1H, Ar-H), 8.33 (s, 1H, Ar-H), 10.09 (s, 1H, OH), 12.19 (s, 1H, N-H). ^{13}C NMR (75 MHz, DMSO-d_6): $\delta = 106.2$, 116.6, 120.0, 120.6, 126.0, 127.6, 130.2, 131.1, 131.4, 131.9, 135.7, 140.0, 148.5, 156.4, 168.7. HRMS (m/z): $[M + H]^+$: Calcd. for $C_{16}H_{11}Cl_2N_3OS$: 364.0073, found: 364.0062.

2-[2-(3-Hydroxybenzylidene)hydrazinyl]-4-(3,4-dichlorophenyl)thiazole (2h)

Yield 61%, m.p. 251–252 °C. IR (ATR): ν_{max} (cm^{-1}) = 3132–3070 (O-H and N-H stretching band), 1624–1598 (C = N and C = C stretching band), 891–761 (1,3-disubstituted and 1,3,4-trisubstituted benzene out-of-plane bending bands). ^{1}H NMR (300 MHz, DMSO-d_6): $\delta = 6.79$ (dt, $J = 8.1$ Hz, 2.0 Hz, 1H, benzene 4-H), 7.04 (d, $J = 7.7$ Hz, 1H, benzene 6-H), 7.11 (s, 1H, thiazole 5-H), 7.22 (t, $J = 7.8$ Hz, 1H, benzene 5-H), 7.52 (s, 1H, benzene 2-H), 7.64 (d, $J = 8.4$ Hz, 1H, benzene 5-H), 7.82 (dd, $J = 8.0$ Hz, 1.9 Hz, 1H, benzene 6-H), 7.95 (s, 1H, benzene 2-H), 8.06 (s, 1H, CH=N), 9.62 (s, 1H, OH), 12.17 (br s, 1H, N-H). ^{13}C NMR (75 MHz, DMSO-d_6): $\delta = 106.3$, 112.5, 112.8, 117.2, 118.5, 118.8, 126.0, 126.8, 127.6, 130.2, 130.3, 131.0, 131.3, 131.9, 135.7, 136.0, 142.2, 148.4, 158.1, 168.9. HRMS (m/z): $[M + H]^+$: Calcd. for $C_{16}H_{11}Cl_2N_3OS$: 364.0077, found: 364.0073.

Biochemistry

Anticholinesterase activity studies

Anticholinesterase activities of the synthesized final compounds were carried out on AChE and BChE enzymes according to the modified Ellman method [52]. A solution (2%) in DMSO of AChE or BChE (20 µL) in the concentration range of 10^{-1}–10^{-6} mM and a solution of the compound (20 µL) was added to 140 µL of phosphate buffer (pH 8 ± 0.1) and incubated at 25 °C for 5 min. The reaction was started by adding 5-5-dithiobis(2-nitrobenzoic acid) (DTNB) (20 µL) and acetylthiocholine iodide ATC (10 µL) to the enzyme-inhibitor mixture. All solutions used in this enzymatic assay were stored at −20 °C and were brought to room temperature just prior to performing the experiments. After mixing the solutions in the wells they were incubated in the oven for 15 min; the absorbance value was 412 nm. The tests were performed at concentrations of 10^{-3} M and 10^{-4} M and the experiments were repeated four times.

Monoamine oxidase inhibition studies

The MAO enzyme inhibitory activity of synthesized final compounds was tested by fluorometric method [53]. The MAO enzyme inhibitory activity of the compounds was investigated by measuring their effects on hydrogen peroxide (H_2O_2) production from tyramine using the Ampliflu Red MAO assay and recombinant hMAO isoforms. H_2O_2 production catalyzed by MAO isoforms can be detected using Ampliflu Red reagent, a non-fluorescent and highly sensitive probe that reacts with H_2O_2 [54]. The synthesized compounds and reference agents were prepared at concentrations of 10^{-3}–10^{-4} M in 2% DMSO. Recombinant hMAO-A (0.5 U/mL) and recombinant hMAO-B (0.64 U/mL) enzymes were dissolved in phosphate buffer and their final volume was made up to 10 mL. Horseradish peroxidase (200 U/mL, 100 µL), Ampliflu Red (20 mM, 200 µL), and tyramine (100 mM, 200 µL) were dissolved in phosphate buffer and made up to 10 mL in final volumes. Solutions of inhibitor (20 µL/well) and hMAO-A (100 µL/well) or hMAO-B (100 µL/well) were added to a plain black bottom 96-well micro-test plate and incubated at 37 °C for 30 min. Solutions of inhibitor (20 µL/well) and hMAO-A (100 µL/well) or hMAO-B (100 µL/well) were added to the 96-well microtest plate and incubated at 37 °C for 30 min. After this incubation period, the reaction was started by adding a working solution (100 µL/well), the mixture was incubated at 37 °C for 30 min, and fluorescence (Ex/Em = 535/587 nm) was measured at 5-min intervals.

In silico method

Molecular docking and molecular dynamics simulation studies were carried out in the same way as in our previous studies [20].

Supporting information

Analytical data (HRMS, ^{1}H NMR and ^{13}C NMR spectra, IR spectra) of the compounds prepared are available in the Supplemental Materials. The dynamics of the protein-ligand interactions are available as a video (MPEG).

Disclosure statement

The author confirms that this article's content has no conflict of interest.

Acknowledgments

We gratefully thank Anadolu University BİBAM and DOPNA Laboratory, where the spectroscopic analyses of the compounds were performed. This study contains parts of the thesis entitled Tutuş [55].

ORCID

Beyzanur Tutuş http://orcid.org/0000-0003-4038-8823
Asaf Evrim Evren http://orcid.org/0000-0002-8651-826X
Begüm Nurpelin Sağlik Özkan http://orcid.org/0000-0002-0151-6266
Leyla Yurttaş http://orcid.org/0000-0002-0957-6044

References

[1] Talesa, V. N. Acetylcholinesterase in Alzheimer's Disease. *Mech. Ageing Dev.* **2001**, *122*, 1961–1969. DOI: 10.1016/S0047-6374(01)00309-8.
[2] Oliveira, C.; Bagetta, D.; Cagide, F.; Teixeira, J.; Amorim, R.; Silva, T.; Garrido, J.; Remião, F.; Uriarte, E.; Oliveira, P. J.; et al. Benzoic Acid-Derived Nitrones: A New Class of Potential Acetylcholinesterase Inhibitors and Neuroprotective Agents. *Eur. J. Med. Chem.* **2019**, *174*, 116–129. DOI: 10.1016/j.ejmech.2019.04.026.
[3] Colovic, M. B.; Krstic, D. Z.; Lazarevic-Pasti, T. D.; Bondzic, A. M.; Vasic, V. M. Acetylcholinesterase Inhibitors: Pharmacology and Toxicology. *Curr. Neuropharmacol.* **2013**, *11*, 315–335. DOI: 10.2174/1570159X11311030006.
[4] Darvesh, S.; Hopkins, D. A.; Geula, C. Neurobiology of Butyrylcholinesterase. *Nat. Rev. Neurosci.* **2003**, *4*, 131–138. DOI: 10.1038/nrn1035.
[5] Lane, R. M.; Potkin, S. G.; Enz, A. Targeting Acetylcholinesterase and Butyrylcholinesterase in Dementia. *Int. J. Neuropsychopharmacol.* **2006**, *9*, 101–124. DOI: 10.1017/S1461145705005833.
[6] Volz, H.-P.; Gleiter, C. H. Monoamine Oxidase Inhibitors. A Perspective on Their Use in the Elderly. *Drugs Aging.* **1998**, *13*, 341–355. DOI: 10.2165/00002512-199813050-00002.
[7] Shulman, K. I.; Herrmann, N.; Walker, S. E. Current Place of Monoamine Oxidase Inhibitors in the Treatment of Depression. *CNS Drugs.* **2013**, *27*, 789–797. DOI: 10.1007/S40263-013-0097-3.
[8] Holschneider, D. P.; Chen, K.; Seif, I.; Shih, J. C. Biochemical, Behavioral, Physiologic, and Neurodevelopmental Changes in Mice Deficient in Monoamine Oxidase A or B. *Brain Res. Bull.* **2001**, *56*, 453–462. DOI: 10.1016/S0361-9230(01)00613-X.
[9] Yamada, M.; Yasuhara, H. Clinical Pharmacology of MAO Inhibitors: Safety and Future. *Neurotoxicology* **2004**, *25*, 215–221. DOI: 10.1016/S0161-813X(03)00097-4.
[10] Kumar, B.; Dwivedi, A. R.; Arora, T.; Raj, K.; Prashar, V.; Kumar, V.; Singh, S.; Prakash, J.; Kumar, V. Design, Synthesis, and Pharmacological Evaluation of *N*-Propargylated Diphenylpyrimidines as Multitarget Directed Ligands for the

Treatment of Alzheimer's Disease. *ACS Chem. Neurosci.* **2022**, *13*, 2122–2139. DOI: 10.1021/acschemneuro.2c00132.

[11] Romero, A.; Cacabelos, R.; Oset-Gasque, M. J.; Samadi, A.; Marco-Contelles, J. Novel Tacrine-Related Drugs as Potential Candidates for the Treatment of Alzheimer's Disease. *Bioorg. Med. Chem. Lett.* **2013**, *23*, 1916–1922. DOI: 10.1016/J.BMCL.2013.02.017.

[12] Nirogi, R.; Shinde, A.; Kambhampati, R. S.; Mohammed, A. R.; Saraf, S. K.; Badange, R. k.; Bandyala, T. R.; Bhatta, V.; Bojja, K.; Reballi, V.; et al. Development of 1-[(2-Bromophenyl)Sulfonyl]-5-Methoxy-3-[(4-Methyl-1-Piperazinyl)Methyl]-1H-Indole Dimesylate Monohydrate (SUVN-502): A Novel, Potent, Selective and Orally Active Serotonin 6 (5-HT6) Receptor Antagonist for Potential Treatment of Alzheimer's Disease. *J. Med. Chem.* **2017**, *60*, 1843–1859. DOI: 10.1021/acs.jmedchem.6b01662.

[13] Zhou, Y.; Fu, Y.; Yin, W.; Li, J.; Wang, W.; Bai, F.; Xu, S.; Gong, Q.; Peng, T.; Hong, Y.; et al. Kinetics-Driven Drug Design Strategy for Next-Generation Acetylcholinesterase Inhibitors to Clinical Candidate. *J. Med. Chem.* **2021**, *64*, 1844–1855. DOI: 10.1021/acs.jmedchem.0c01863.

[14] Scheltens, P.; De Strooper, B.; Kivipelto, M.; Holstege, H.; Chételat, G.; Teunissen, C. E.; Cummings, J.; van der Flier, W. M. Alzheimer's Disease. *Lancet* **2021**, *397*, 1577–1590. DOI: 10.1016/S0140-6736(20)32205-4.

[15] Enz, A.; Amstutz, R.; Boddeke, H.; Gmelin, G.; Malanowski, J. Chapter 53: Brain Selective Inhibition of Acetylcholinesterase: A Novel Approach to Therapy for Alzheimer's Disease. *Prog. Brain Res.* **1993**, *98*, 431–438. DOI: 10.1016/S0079-6123(08)62429-2.

[16] Hampel, H.; Mesulam, M.-M.; Cuello, A. C.; Farlow, M. R.; Giacobini, E.; Grossberg, G. T.; Khachaturian, A. S.; Vergallo, A.; Cavedo, E.; Snyder, P. J.; et al. The Cholinergic System in the Pathophysiology and Treatment of Alzheimer's Disease. *Brain* **2018**, *141*, 1917–1933. DOI: 10.1093/BRAIN/AWY132.

[17] Chin-Chan, M.; Navarro-Yepes, J.; Quintanilla-Vega, B. Environmental Pollutants as Risk Factors for Neurodegenerative Disorders: Alzheimer and Parkinson Diseases. *Front. Cell. Neurosci.* **2015**, *9*, 124. DOI: 10.3389/fncel.2015.00124.

[18] Mathew, B.; Parambi, D. G. T.; Mathew, G. E.; Uddin, M. S.; Inasu, S. T.; Kim, H.; Marathakam, A.; Unnikrishnan, M. K.; Carradori, S. Emerging Therapeutic Potentials of Dual-Acting MAO and AChE Inhibitors in Alzheimer's and Parkinson's Diseases. *Arch. Pharm.* **2019**, *352*, 1900177. DOI: 10.1002/ardp.201900177.

[19] Kumar, B.; Kumar, V.; Prashar, V.; Saini, S.; Dwivedi, A. R.; Bajaj, B.; Mehta, D.; Parkash, J.; Kumar, V. Dipropargyl Substituted Diphenylpyrimidines as Dual Inhibitors of Monoamine Oxidase and Acetylcholinesterase. *Eur. J. Med. Chem.* **2019**, *177*, 221–234. DOI: 10.1016/j.ejmech.2019.05.039.

[20] Al-Sharabi, A. A.; Evren, A. E.; Sağlık, B. N.; Yurttaş, L. Synthesis, Characterization, Molecular Docking and Molecular Dynamics Simulations of Novel 2,5-Disubstituted-1,3,4-Thiadiazole Derivatives as Potential Cholinesterase/Monoamine Oxidase Dual Inhibitors for Alzheimer's Disease. *J. Biomol. Struct. Dyn.* **2023**, 1–19. DOI: 10.1080/07391102.2023.2274967.

[21] Zhong, G.; Guo, J.; Pang, C.; Su, D.; Tang, C.; Jing, L.; Zhang, F.; He, P.; Yan, Y.; Chen, Z.; et al. Novel AP2238-Clorgiline Hybrids as Multi-Target Agents for the Treatment of Alzheimer's Disease: Design, Synthesis, and Biological Evaluation. *Bioorg. Chem.* **2023**, *130*, 106224. DOI: 10.1016/j.bioorg.2022.106224.

[22] Zha, G. F.; Leng, J.; Darshini, N.; Shubhavathi, T.; Vivek, H. K.; Asiri, A. M.; Marwani, H. M.; Rakesh, K. P.; Mallesha, N.; Qin, H. L. Synthesis, SAR and Molecular Docking Studies of Benzo[*d*]thiazole-Hydrazones as Potential Antibacterial and Antifungal Agents. *Bioorg. Med. Chem. Lett.* **2017**, *27*, 3148–3155. DOI: 10.1016/j.bmcl.2017.05.032.

[23] Bueno, J. M.; Carda, M.; Crespo, B.; Cuñat, A. C.; de Cozar, C.; León, M. L.; Marco, J. A.; Roda, N.; Sanz-Cervera, J. F. Design, Synthesis and Antimalarial Evaluation of Novel Thiazole Derivatives. *Bioorg. Med. Chem. Lett.* **2016**, *26*, 3938–3944. DOI: 10.1016/j.bmcl.2016.07.010.

[24] Karale, U. B.; Krishna, V. S.; Krishna, E. V.; Choudhari, A. S.; Shukla, M.; Gaikwad, V. R.; Mahizhaveni, B.; Chopra, S.; Misra, S.; Sarkar, D.; et al. Synthesis and Biological Evaluation of 2,4,5-Trisubstituted Thiazoles as Antituberculosis Agents Effective against Drug-Resistant Tuberculosis. *Eur. J. Med. Chem.* **2019**, *178*, 315–328. DOI: 10.1016/j.ejmech.2019.05.082.

[25] Yeh, T. K.; Kang, I. J.; Hsu, T. A.; Lee, Y. C.; Lee, C. C.; Hsu, S. J.; Tian, Y. W.; Yang, H. Y.; Chen, C. T.; Chao, Y. S.; et al. A Novel, Potent, and Orally Bioavailable Thiazole HCV NS5A Inhibitor for the Treatment of Hepatitis C Virus. *Eur. J. Med. Chem.* **2019**, *167*, 245–268. DOI: 10.1016/j.ejmech.2019.02.016.

[26] Jacob, J. P; Manju, S. L. Identification and Development of Thiazole Leads as COX-2/5-LOX Inhibitors through *in-Vitro* and *in-Vivo* Biological Evaluation for Anti-Inflammatory Activity. *Bioorg. Chem.* **2020**, *100*, 103882. DOI: 10.1016/j.bioorg.2020.103882.

[27] Sever, B.; Altıntop, M. D.; Demir, Y.; Akalın Çiftçi, G.; Beydemir, Ş.; Özdemir, A. Design, Synthesis, *in Vitro* and *in Silico* Investigation of Aldose Reductase Inhibitory Effects of New Thiazole-Based Compounds. *Bioorg. Chem.* **2020**, *102*, 104110. DOI: 10.1016/j.bioorg.2020.104110.

[28] Łączkowski, K. Z.; Sałat, K.; Misiura, K.; Podkowa, A.; Malikowska, N. Synthesis and Anticonvulsant Activities of Novel 2-(Cyclopentylmethylene)Hydrazinyl-1,3-Thiazoles in Mouse Models of Seizures. *J. Enzyme Inhib. Med. Chem.* **2016**, *31*, 1576–1582. DOI: 10.3109/14756366.2016.1158172.

[29] Adole, V. A.; More, R. A.; Jagdale, B. S.; Pawar, T. B.; Chobe, S. S. Efficient Synthesis, Antibacterial, Antifungal, Antioxidant and Cytotoxicity Study of 2-(2-Hydrazineyl)Thiazole Derivatives. *ChemistrySelect* **2020**, *5*, 2778–2786. DOI: 10.1002/slct.201904609.

[30] de Santana, T. I.; Barbosa, M. D O.; Gomes, P. A. T. D M.; da Cruz, A. C. N.; da Silva, T. G.; Leite, A. C. L. Synthesis, Anticancer Activity and Mechanism of Action of New Thiazole Derivatives. *Eur. J. Med. Chem.* **2018**, *144*, 874–886. DOI: 10.1016/j.ejmech.2017.12.040.

[31] Duan, L. M.; Yu, H. Y.; Li, Y. L.; Jia, C. J. Design and Discovery of 2-(4-(1*H*-Tetrazol-5-yl)-1*H*-Pyrazol-1-yl)-4-(4-Phenyl)Thiazole Derivatives as Cardiotonic Agents via Inhibition of PDE3. *Bioorg. Med. Chem.* **2015**, *23*, 6111–6117. DOI: 10.1016/j.bmc.2015.08.002.

[32] Ateş, İO.; Evren, A. E.; Sağlik, B. N.; Yurttaş, L. New Indane Derivatives Containing 2-Hydrazinothiazole as Potential Acetylcholinesterase and Monoamine Oxidase-B Inhibitors. *Z Naturforsch. C. J. Biosci.* **2021**, *76*, *C*, 417–424. DOI: 10.1515/znc-2021-0058.

[33] Evren, A. E.; Nuha, D.; Dawbaa, S.; Sağlık, B. N.; Yurttaş, L. Synthesis of Novel Thiazolyl Hydrazone Derivatives as Potent Dual Monoamine Oxidase-Aromatase Inhibitors. *Eur. J. Med. Chem.* **2022**, *229*, 114097. DOI: 10.1016/j.ejmech.2021.114097.

[34] Chimenti, F.; Secci, D.; Bolasco, A.; Chimenti, P.; Granese, A.; Carradori, S.; MacCioni, E.; Cardia, M. C.; Yáñez, M.; Orallo, F.; et al. Synthesis, Semipreparative HPLC Separation, Biological Evaluation, and 3D-QSAR of Hydrazothiazole Derivatives as Human Monoamine Oxidase B Inhibitors. *Bioorg. Med. Chem.* **2010**, *18*, 5063–5070. DOI: 10.1016/j.bmc.2010.05.070.

[35] Chimenti, F.; Secci, D.; Bolasco, A.; Chimenti, P.; Granese, A.; Carradori, S.; Yáñez, M.; Orallo, F.; Sanna, M. L.; Gallinella, B.; et al. Synthesis, Stereochemical Separation, and Biological Evaluation of Selective Inhibitors of Human MAO-B: 1-(4-Arylthiazol-2-yl)-2-(3- Methylcyclohexylidene)Hydrazines. *J. Med. Chem.* **2010**, *53*, 6516–6520. DOI: 10.1021/jm100120s.

[36] Chimenti, F.; Bolasco, A.; Secci, D.; Chimenti, P.; Granese, A.; Carradori, S.; Yáñez, M.; Orallo, F.; Ortuso, F.; Alcaro, S. Investigations on the 2-Thiazolylhydrazyne Scaffold: Synthesis and Molecular Modeling of Selective Human Monoamine

Oxidase Inhibitors. *Bioorg. Med. Chem.* **2010**, *18*, 5715–5723. DOI: 10.1016/j.bmc.2010.06.007.

[37] Carradori, S.; Ortuso, F.; Petzer, A.; Bagetta, D.; De Monte, C.; Secci, D.; De Vita, D.; Guglielmi, P.; Zengin, G.; Aktumsek, A.; et al. Design, Synthesis and Biochemical Evaluation of Novel Multi-Target Inhibitors as Potential Anti-Parkinson Agents. *Eur. J. Med. Chem.* **2018**, *143*, 1543–1552. DOI: 10.1016/j.ejmech.2017.10.050.

[38] D'Ascenzio, M.; Chimenti, P.; Gidaro, M. C.; De Monte, C.; De Vita, D.; Granese, A.; Scipione, L.; Di Santo, R.; Costa, G.; Alcaro, S.; et al. (Thiazol-2-yl)Hydrazone Derivatives from Acetylpyridines as Dual Inhibitors of MAO and AChE: Synthesis, Biological Evaluation and Molecular Modeling Studies. *J. Enzyme. Inhib. Med. Chem* **2015**, *30*, 908–919. DOI: 10.3109/14756366.2014.987138.

[39] Özkay, Y.; Yurttaş, L.; Mohsen, U. A.; Sever, B.; Hussein, W.; Öztürk, Ö.; Sağlık, B. N.; Acar, U.; Erdoğan, Ö. N.; Pekbağ, A.; et al. Study on Thiazolyl-Hydrazone Derivatives as Acetylcholinesterase Inhibitors. *Clin. Exp. Health Sci.* **2014**, *4*, 38–42. DOI: 10.5455/musbed.20140101090010.

[40] Chimenti, P.; Petzer, A.; Carradori, S.; D'Ascenzio, M.; Silvestri, R.; Alcaro, S.; Ortuso, F.; Petzer, J. P.; Secci, D. Exploring 4-Substituted-2-Thiazolylhydrazones from 2-, 3-, and 4-Acetylpyridine as Selective and Reversible HMAO-B Inhibitors. *Eur. J. Med. Chem.* **2013**, *66*, 221–227. DOI: 10.1016/j.ejmech.2013.05.032.

[41] Chimenti, F.; Maccioni, E.; Secci, D.; Bolasco, A.; Chimenti, P.; Granese, A.; Befani, O.; Turini, P.; Alcaro, S.; Ortuso, F.; et al. Selective Inhibitory Activity against MAO and Molecular Modeling Studies of 2-Thiazolylhydrazone Derivatives. *J. Med. Chem.* **2007**, *50*, 707–712. DOI: 10.1021/jm060869d.

[42] Distinto, S.; Yáñez, M.; Alcaro, S.; Cardia, M. C.; Gaspari, M.; Sanna, M. L.; Meleddu, R.; Ortuso, F.; Kirchmair, J.; Markt, P.; et al. Synthesis and Biological Assessment of Novel 2-Thiazolylhydrazones and Computational Analysis of Their Recognition by Monoamine Oxidase B. *Eur. J. Med. Chem.* **2012**, *48*, 284–295. DOI: 10.1016/j.ejmech.2011.12.027.

[43] Daina, A.; Michielin, O.; Zoete, V. SwissADME: A Free Web Tool to Evaluate Pharmacokinetics, Drug-Likeness and Medicinal Chemistry Friendliness of Small Molecules. *Sci. Rep.* **2017**, *7*, 42717. DOI: 10.1038/srep42717.

[44] Potts, R. O.; Guy, R. H. Predicting Skin Permeability. *Pharm. Res.* **1992**, *9*, 663–669. DOI: 10.1023/A:1015810312465.

[45] Schaffer, N. K.; Michel, H. O.; Bridges, A. F. Amino Acid Sequence in the Region of the Reactive Serine Residue of Eel Acetylcholinesterase. *Biochemistry* **1973**, *12*, 2946–2950. DOI: 10.1021/bi00739a027.

[46] Adelusi, T. I.; Oyedele, A. Q. K.; Boyenle, I. D.; Ogunlana, A. T.; Adeyemi, R. O.; Ukachi, C. D.; Idris, M. O.; Olaoba, O. T.; Adedotun, I. O.; Kolawole, O. E.; et al. Molecular Modeling in Drug Discovery. *Inform. Med. Unlocked* **2022**, *29*, 100880. DOI: 10.1016/j.imu.2022.100880.

[47] Al-Sharabi, A. A.; Saffour, S.; Evren, A. E.; Bayazıt, G.; Çongur, G.; Gül, Ü. D.; Yurttaş, L. Synthesis, Antimicrobial Activity, Electrochemical Studies and Molecular Modeling Studies of Novel 1,3,4-Oxadiazole Derivatives. *J. Mol. Struc.* **2023**, *1289*, 135775. DOI: 10.1016/j.molstruc.2023.135775.

[48] Boroushaki, T.; Dekamin, M. G. Interactions between β-Cyclodextrin as a Carrier for Anti-Cancer Drug Delivery: A Molecular Dynamics Simulation Study. *J. Biomol. Struct. Dyn.* **2023**, *41*, 11551–11563. DOI: 10.1080/07391102.2022.2164058.

[49] Surti, M.; Patel, M.; Adnan, M.; Moin, A.; Ashraf, S. A.; Siddiqui, A. J.; Snoussi, M.; Deshpande, S.; Reddy, M. N. Ilimaquinone (Marine Sponge Metabolite) as a Novel Inhibitor of SARS-CoV-2 Key Target Proteins in Comparison with Suggested COVID-19 Drugs: Designing, Docking and Molecular Dynamics Simulation Study. *RSC Adv.* **2020**, *10*, 37707–37720. DOI: 10.1039/D0RA06379G.

[50] Osmaniye, D.; Evren, A. E.; Karaca, Ş.; Özkay, Y.; Kaplancıklı, Z. A. Novel Thiadiazol Derivatives; Design, Synthesis, Biological Activity, Molecular Docking and Molecular Dynamics. *J. Mol. Struct.* **2023**, *1272*, 134171. DOI: 10.1016/j.molstruc.2022.134171.

[51] Li, S.; Luan, G.; Ren, X.; Song, W.; Xu, L.; Xu, M.; Zhu, J.; Dong, D.; Diao, Y.; Liu, X.; et al. Rational Design of Benzylidenehydrazinyl-Substituted Thiazole Derivatives as Potent Inhibitors of Human Dihydroorotate Dehydrogenase with *in Vivo* Anti-Arthritic Activity. *Sci. Rep.* **2015**, *5*, 14836. DOI: 10.1038/srep14836.

[52] Ellman, G. L.; Courtney, K. D.; Andres, V.; Featherstone, R. M. A New and Rapid Colorimetric Determination of Acetylcholinesterase Activity. *Biochem. Pharmacol.* **1961**, *7*, 88–95. DOI: 10.1016/0006-2952(61)90145-9.

[53] Sağlık, B. N.; Kaya Çavuşoğlu, B.; Osmaniye, D.; Levent, S.; Acar Çevik, U.; Ilgın, S.; Özkay, Y.; Kaplancıklı, Z. A.; Öztürk, Y. *In Vitro* and *in Silico* Evaluation of New Thiazole Compounds as Monoamine Oxidase Inhibitors. *Bioorg. Chem.* **2019**, *85*, 97–108. DOI: 10.1016/j.bioorg.2018.12.019.

[54] Carradori, S.; D'Ascenzio, M.; De Monte, C.; Secci, D.; Yáñez, M. Synthesis and Selective Human Monoamine Oxidase B Inhibition of Heterocyclic Hybrids Based on Hydrazine and Thiazole Scaffolds. *Arch. Pharm.* **2013**, *346*, 17–22. DOI: 10.1002/ardp.201200318.

[55] Tutuş, B. Synthesis of new 2-hydrazinothiazole derivatives and investigation of their biological effects. **2022**. Master's Thesis, Institute of Graduate Education, Anadolu University, Eskişehir, Turkey.